Effects of correcting salinity with altimeter measurements in an equatorial Pacific ocean model

Femke C. Vossepoel[1]
Delft Institute for Earth-Oriented Space Research (DEOS), Delft University of Technology, Delft, Netherlands

Gerrit Burgers
Royal Netherlands Meteorological Institute (KNMI), De Bilt, Netherlands

Peter Jan van Leeuwen
Institute for Marine and Atmospheric Research Utrecht (IMAU), Utrecht University, Utrecht, Netherlands

Received 29 January 2001; revised 24 January 2002; accepted 4 February 2002; published 18 September 2002.

[1] In this paper, we study the consequences of making salinity corrections in a tropical Pacific ocean model run for the period 1993–1997. Salinity and temperature corrections are obtained by assimilating temperature profile data and TOPEX/Poseidon sea level observations in the ocean general circulation model of the National Centers for Environmental Prediction (NCEP). The results are compared to two model runs in which no salinity corrections have been made, one using only temperature data and the other using both temperature and sea level data. The salinity correction sharpens the salinity front at the eastern edge of the western Pacific fresh pool, leading to improved patterns of salinity variability in the model. In addition, the salinity correction allows the model to follow both the temperature and the sea level more closely and estimates the heat content more accurately compared to the case when only temperature is corrected. In the western Pacific, the zonal pressure gradient resulting from the combined temperature and salinity corrections causes an acceleration of the Equatorial Under Current (EUC) that differs from the case when correcting temperature only. In the eastern Pacific, zonal current changes are similar for both runs in which sea level has been assimilated, and are directly related to local changes in surface pressure. We do not observe a remote effect of the salinity corrections on the zonal current structure in the eastern Pacific. *INDEX TERMS:* 4556 Oceanography: Physical: Sea level variations; 4512 Oceanography: Physical: Currents; 4203 Oceanography: General: Analytical modeling; 4231 Oceanography: General: Equatorial oceanography

Citation: Vossepoel, F. C., G. Burgers, and P. J. van Leeuwen, Effects of correcting salinity with altimeter measurements in an equatorial Pacific ocean model, *J. Geophys. Res.*, *107*(C12), 8001, doi:10.1029/2001JC000816, 2002.

1. Introduction

[2] The evolution of El Niño in the tropical Pacific Ocean is simulated with great accuracy by a number of Ocean General Circulation Models (OGCMs) (for an overview, see *Stockdale et al.* [1998]). The performance of these OGCMs is generally evaluated in terms of their ability to simulate temperature variability. While the assimilation of temperature data generally improves the simulation of temperature variability, it may worsen the simulation of salinity variability.

[3] The basic features of salinity variability in the tropical Pacific are well known. The warm pool region in the western Pacific is characterized by relatively fresh surface waters (salinity lower than 34.8 psu), the so-called "fresh pool" [*Delcroix and Picaut*, 1998]. The zonal displacements of this fresh pool are in phase with the zonal displacements of the warm pool. A detailed description of salinity variability in this region can be found in the papers by *Delcroix et al.* [1996], *Delcroix and Picaut* [1998] and *Vialard and Delecluse* [1998a, 1998b]. The salinity variability affects the circulation through density effects, in particular through horizontal pressure gradients [*Cooper*, 1988; *Murtugudde and Busalacchi*, 1998; *Roemmich et al.*, 1994] and vertical mixing effects [*Godfrey and Lindstrom*, 1989; *Lukas and Lindstrom*, 1991; *Shinoda and Lukas*, 1995; *Ando and McPhaden*, 1997]. The relative impact of these two effects on the ocean analysis of an OGCM is presented by *Vialard et al.* [2002].

[4] Several methods have been developed to assimilate salinity in ocean models. As salinity data are sparse, most salinity assimilation methods use indirect observations to

[1]Also at Royal Netherlands Meteorological Institute (KNMI), De Bilt, Netherlands.

0148-0227/02/2001JC000816$09.00

correct the model's salinity field. *Troccoli and Haines* [1999] developed a method that uses temperature observations and temperature–salinity (T–S) relations. *Vossepoel et al.* [1998], *Maes and Behringer* [2000], and *Maes et al.* [2000] developed methods that estimate salinity based on temperature observations, sea level observations, and T–S relations. Although it is hardly possible to reconstruct the full complexity of the salinity variability without direct observations of salinity, such methods successfully reconstruct the large-scale interannual salinity variations of the tropical Pacific Ocean. In the current paper, we apply the assimilation method of *Vossepoel and Behringer* [2000], which uses temperature and altimetric sea level data to correct the salinity field. This method assumes that temperature can be estimated accurately in the equatorial Pacific, and that discrepancies between sea level observations and model dynamic height can be attributed to errors in model salinity. The first objective of this paper is to evaluate to what extend this method is able to estimate the mean salinity field and variability in the equatorial Pacific.

[5] In the NCEP analysis, the surface velocities in the western Pacific are too strong, and sometimes in a direction opposite to observed values [*Halpern et al.*, 1995, 1998; *Acero-Schertzer et al.*, 1997; *Behringer et al.*, 1998]. In fact, *Acero-Schertzer et al.* [1997] suggested that discrepancies in the model's surface velocity field may be related to errors in the salinity field, implying that salinity corrections could lead to improved surface currents. To investigate the dynamical impact of salinity corrections (both at the surface and below) is the second objective of this paper.

[6] In our case salinity correction is obtained from sea level information, and changes the density field closer to the surface than when sea level information were translated to a temperature correction. What consequences does this have for the resulting ocean analysis? More specifically, does a salinity correction lead to a better model representation of the mean ocean state, and of the simulation of heat- and salt content, and what is the impact on the equatorial current variability? The importance of these questions is evident, as with large data assimilation projects (e.g., GODAE, Mercator) and expanding observational activities (SMOS, Argo floats) the possibilities of implementing salinity data assimilation in (operational) ocean models will increase.

[7] We study the impact of salinity changes by comparing three runs for the period 1993–1997. In the first run we assimilate temperature observations and correct temperature. Both the second and the third run assimilate temperature and dynamic height observations. In the second run, we only correct temperature, while in the third run we correct temperature and salinity changes following *Vossepoel et al.* [1998]. Given the same observations, the second and third run allow us to isolate the effect of salinity corrections. In an additional run, we study the local and remote effects of the different data assimilation corrections along the equator by limiting the region in which data are assimilated.

[8] The structure of this paper is as follows. First, a brief description of the model and assimilation scheme as well as the data sets that are used for verification is presented in section 2. Section 3 describes the four-year mean model fields of the two assimilation runs, focusing on dynamic height, sea surface salinity (SSS) and zonal velocity. Next, section 4 describes the variability of these fields. Section 5 gives a summary of results obtained in this study, and discusses implications for ocean modeling.

2. Model, Assimilation Schemes, and Data

[9] The ocean analysis system used in this study consists of a primitive equations ocean model and a variational assimilation scheme. Both the model and the assimilation scheme are briefly described in the paper by *Vossepoel and Behringer* [2000]. A more detailed description of the ocean analysis system can be found in the works of *Ji et al.* [1995] and *Behringer et al.* [1998].

2.1. Ocean Model

[10] The model is based on the Modular Ocean Model (MOM, version 1), developed at Geophysical Fluid Dynamics Laboratory [*Bryan*, 1969; *Cox*, 1984; *Philander et al.*, 1987], and is similar to the version that is used at NCEP in operational ENSO forecasting. The model domain extends from 120°E to 70°W, with a 1.5° zonal resolution. Latitudinal resolution in the region between 10°S and 10°N is 1/3°, gradually increasing to 1° poleward of 20° latitude. The model has 28 levels, 18 of them concentrated in the top 400 meters. Mixing is based on the scheme of *Pacanowski and Philander* [1981]. In this mixing scheme, the vertical eddy viscosity and diffusivity are dependent on the Richardson number.

[11] In the original model used by *Behringer et al.* [1998], the salinity variability was relatively low. In our version of the NCEP ocean model [*Vossepoel and Behringer*, 2000], salinity variability is increased by adding a term to the prognostic salinity equation that relaxes the model salinity to estimates based on climatological T–S correlations from *Levitus and Boyer* [1994] and *Levitus et al.* [1994]. The time scale for this relaxation is 50 days. At the surface, there is no relaxation, but instead a salt flux forcing is applied that consists of an evaporation minus precipitation estimate. This field is composed of a climatological average of the 1979–1995 composite precipitation data, known as the Climate Prediction Center Merged Analysis of Precipitation (CMAP) of *Xie and Arkin* [1997], combined with an average for the same period of the evaporation fields from the atmospheric reanalysis of the National Centers for Environmental Prediction (NCEP) [*Kalnay et al.*, 1996]. Wind forcing is derived from the pseudo-stress wind fields of the Florida State University [*Stricherz et al.*, 1992].

2.2. Data Assimilation Schemes

[12] In this study, we apply the original, univariate scheme as used by *Behringer et al.* [1998] and two modified schemes that assimilate sea level observations. The first scheme is the original NCEP scheme which is derived from the variational scheme of *Derber and Rosati* [1989]. This univariate scheme corrects temperature only, by assimilating temperature observations. The cost function for this scheme is described by *Behringer et al.* [1998]. The temperature observations for both runs are obtained from Voluntary Observing Ships (VOS) and TAO moorings. The model run with this scheme will be denoted as the univariate Real Temperature assimilation run (RT1).

[13] The second scheme, also a univariate scheme that corrects temperature only, assimilates both temperature observations and surface dynamic heights as given by TOPEX/Poseidon (T/P) observations. This is accomplished by adding an extra surface dynamic height term to the observational part of the cost function. To be consistent with *Ji et al.* [2000], T/P deviations from the mean over 1993–1995 are compared in the cost function to model dynamic height deviations from a dynamic height relative to 500 meters depth that is computed with *Levitus and Boyer* [1994] and *Levitus et al.* [1994] profiles. The model run with this scheme will be denoted as the univariate Real Temperature and Dynamic height assimilation run (RTD1).

[14] The third scheme is the bivariate scheme of *Vossepoel et al.* [1998] that corrects both temperature and salinity. It uses the same observations and observational term in the cost function as RTD1. Given the dense coverage of temperature observations in the equatorial Pacific ocean, assimilation of temperature observations guarantees a relatively good reconstruction of temperature variability and associated changes in dynamic height. Remaining dynamic height differences can be largely attributed to errors in model salinity variability. To correct these errors the bivariate method uses a model error-covariance matrix that is based on empirical correlations between dynamic height and (sub)surface salinity changes [*Vossepoel et al.*, 1998]. The shape of this error-covariance matrix favors salinity corrections in the upper layers of the ocean to those below the thermocline. The method only takes into account baroclinic sea level variations, assuming that barotropic sea level variations are negligible. Further details on the developing and testing of this scheme can be found in the work of *Vossepoel and Behringer* [2000]. The model run with this scheme will be denoted as the bivariate Real Temperature and Dynamic height assimilation run (RTD2).

2.3. Salinity Data for Verification

[15] Direct salinity observations are not assimilated in any of the runs described in the current paper, but are used for testing instead. The available data set of direct salinity observations partly overlaps with the set of *Delcroix et al.* [1996]. Three types of observations are combined in this observational data set: thermosalinograph and bucket observations from the Institut de Recherche pour le Développement (IRD, previously ORSTOM, New Caledonia, provided by Chr. Hénin), and conductivity–temperature–depth (CTD) observations from the Pacific Marine Environmental Laboratory (PMEL, provided by M. McPhaden). Analyses of these observations can be found in the works of *Ando and McPhaden* [1997], *Cronin and McPhaden* [1998] (CTD), *Delcroix and Picaut* [1998] (bucket and thermosalinograph), and *Hénin et al.* [1998].

[16] Salinity observations from the CTD profiles have been averaged in 5-meter bins, and the 0–5 meter depth bin is used as a proxy for sea surface salinity. This is done because the observations contain traces of high-frequency small-scale processes such as rain squalls, which the model is unable to reproduce. By averaging the upper 5 meters in one bin, we smooth the effects of these processes [cf. *Vossepoel et al.*, 1998].

3. Four-Year Mean Analyses (1993–1997)

3.1. Dynamic Height

[17] Not surprisingly, assimilation of T/P observations affects the model simulation of dynamic height. The mean dynamic height field for 1993–1997 is clearly affected by the salinity corrections in RTD2: the dynamic height of RTD2 is around 5 dyn cm higher in the fresh pool of RTD2 than in that of RT1 (results not shown). This difference is centered at 8°N between 130°E and the dateline. In contrast, the mean dynamic height in the region of the surface salinity maximum in the southern hemisphere is almost 15 dyn cm lower in RTD2 than in RT1 (for simplicity, we will replace dyn cm by cm in the following). Patterns in the RTD2-RT1 dynamic height difference coincide with RTD2-RT1 SSS differences. The RTD1-RT1 dynamic height differences are similar to RTD2-RT1, but instead are related to temperature differences, mostly at thermocline depth.

3.2. Sea Surface Salinity

[18] Figure 1 illustrates the differences between the mean SSS of RTD2 and RT1. The RTD1 SSS field is very similar to RT1, and will therefore not be discussed separately. As a result of the relaxation to climatological T–S relations, SSS in RT1 shows some contrast between the fresh pool in the western equatorial Pacific (around 34.5 psu) and the saltier waters in the southern central Pacific (around 35 psu). The span is much larger in RTD2, and is probably overestimated (cf. the observations of *Delcroix et al.* [1996] over the period 1969–1994). While in the western Pacific (around 8°N) the differences between RTD2 and RT1 are relatively small, in the east, near the coast of Costa Rica and near 10°S, 120°W, the RTD2 salinity is closer to *Delcroix et al.* [1996] than the RT1 analysis.

[19] From the three types of observations described in section 2.3, all data between 2°S and 2°N were mapped to study both the mean and the variability of SSS. The observed mean SSS field along the equator is illustrated in Figure 2. The observations are compared with equatorial model SSS, that is obtained from monthly averages of the RTD2 and RT1 output fields. The most striking feature in Figure 2 is the strengthening of the salinity front (around the 35.0 psu isohaline that denotes the eastern edge of the fresh pool). This is a remarkable result because no direct observations of salinity have been used in the assimilation of RTD2.

3.3. Vertical Structure of Salinity Along the Equator

[20] The largest mean salinity differences between RTD2 and RT1 along the equator occur in the western Pacific. The vertical structure of these salinity differences is illustrated with longitude-depth sections in Figure 3. Although the general salinity structure in both model runs is similar, a strong contrast between the relatively low salinity waters in the west and the saltier waters in the central Pacific can be observed in RTD2. This corresponds with a stronger dynamic height gradient at the surface, and weaker surface velocities, as will be shown in section 3.4. The bottom panel of Figure 3 demonstrates that the salinity correction is mostly applied in the upper ocean layers, in accordance with the salinity error covariance matrix in the salinity assimilation method (for details, see *Vossepoel and Beh-*

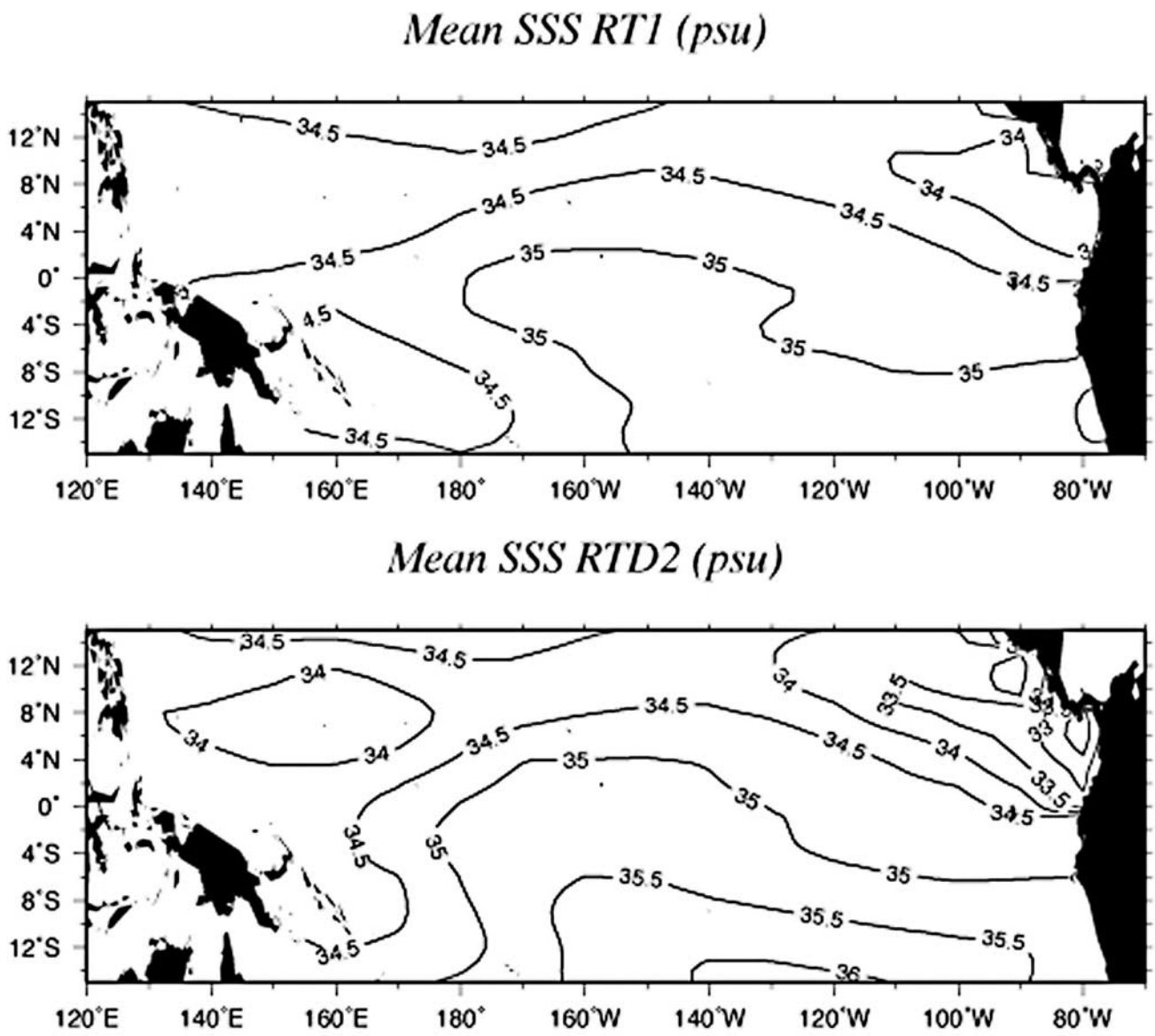

Figure 1. Mean sea surface salinity computed for the period 1993–1997 for RT1 and RTD2.

ringer [2000]). The salinity field of RTD1 is very similar to RT1, and is not discussed separately.

3.4. Vertical Structure of Zonal Velocity

3.4.1. Impact of T/P Assimilation

[21] Figure 4 shows the vertical slice of the four-year mean zonal velocities at the equator for the model run without salinity correction (RT1) as well as the RTD1-RT1 and RTD2-RT1 zonal velocity differences. Both RTD1-RT1 and RTD2-RT1 have a positive anomaly close to the surface at the date line as a result of a difference in surface pressure. According to *Wacongne* [1989] and *Wacongne* [1990], the western Pacific is where the Equatorial Under Current (EUC) is accelerated by a zonal pressure gradient, so changes in the zonal pressure gradient in that region will have a direct impact on EUC strength.

[22] In the eastern Pacific, we observe weaker westward surface currents, and a stronger eastward EUC in RTD1 and RTD2 compared to RT1. In addition, the EUC extends to greater depth than further west. We performed an additional model run. This run is similar to RTD2, but assimilated no T/P data east of 160W. The monthly averaged zonal velocity fields of this run are nearly identical to the zonal velocity in RT1. This points to a local generation in the eastern Pacific, rather than a remotely forced response related to changes in the western Pacific.

3.4.2. Impact of Salinity Correction

[23] As sea level and surface pressure are nearly the same for RTD2 and RTD1, the surface currents of both runs are very similar. Below the surface, differences become evident as a result of the difference in density correction. While RTD1-RT1 density differences are located at thermocline depth, RTD2-RT1 density differences are located close to the surface. The implications of this difference in density corrections for the zonal velocity field are depicted in the top panel of Figure 5. Comparing to Figure 3, it becomes clear that the main impact on zonal velocity is near the longitude of the largest salinity correction. The differences

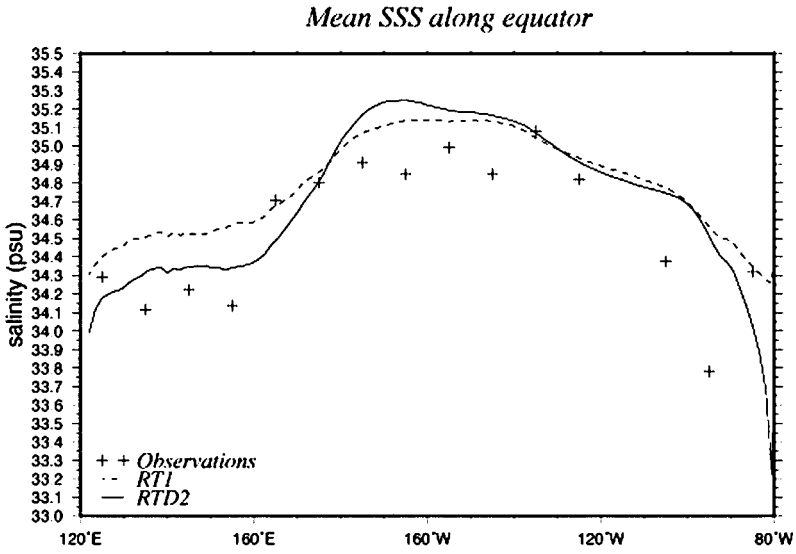

Figure 2. Mean sea surface salinity computed for the period 1993–1997 for RT1 and RTD2 compared to observations along the equator.

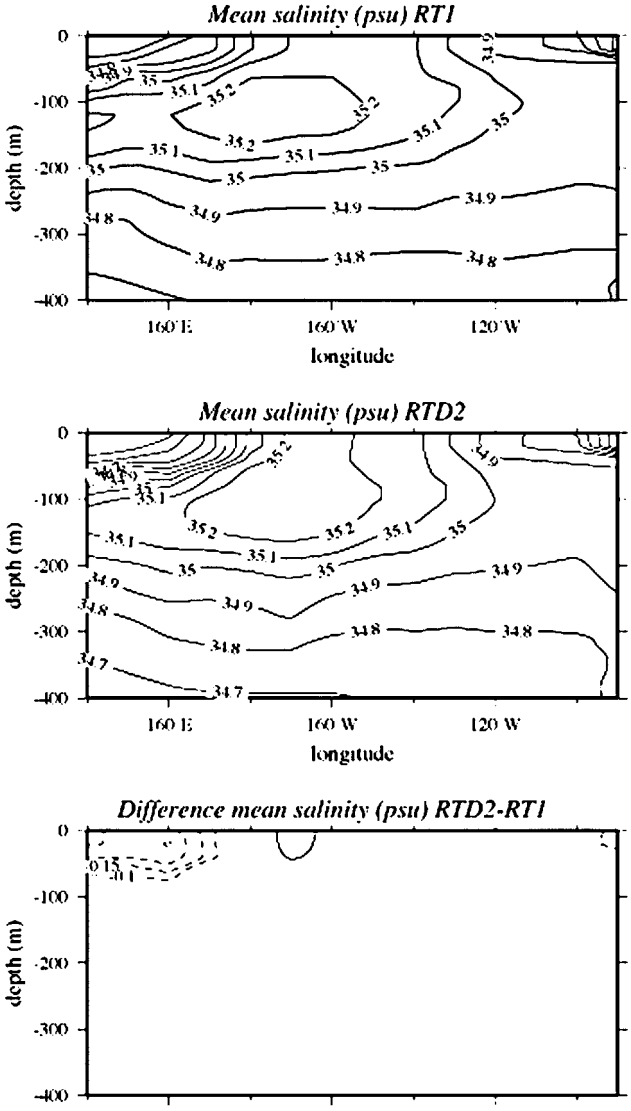

Figure 3. Mean salinity along the equator computed for the period 1993–1997 for RT1 and RTD2.

arise, because in RT1 the difference in surface pressure is balanced by density changes at thermocline depth, causing pressure differences in all layers above thermocline depth, while in RTD2 the density changes are spread out over the thermocline and the layers above, as is illustrated by the difference in zonal pressure gradient depicted in Figure 5. Because the density changes in RTD2 are spread over the thermocline and over the layers above, the resulting zonal pressure gradient is less strong at thermocline depth than in RTD1. Consequently, the acceleration of the RTD2 EUC is stronger west of 160°E than in RTD1.

[24] In the all three runs, equatorial zonal currents are nearly the same as the geostrophic currents calculated from the second meridional derivative of pressure. We observe that the geostrophic adjustment results in slight off-equatorial differences in temperature and salinity in addition to the salinity corrections which are constrained to the upper layers.

[25] Model velocity fields have been compared to current observations from moorings (results not shown). The simulation of surface currents in the western Pacific is rather poor in all three model runs. The mixed layer is too shallow in the western Pacific, and the surface currents are too strong. The mixed-layer depth is not significantly deepened in RTD2 compared to RTD1 or RT1.

4. Variability of the 1993–1997 Period

4.1. Dynamic Height Variability

[26] Figure 6 shows the temporal evolution of dynamic height anomalies along the equator that reflects the evolution of the ENSO events of the 1993–1997 period. RT1 anomalies are computed relative to the average monthly climatology that has been determined from monthly averages for RT1 over the five-year period. Similarly, RTD2 anomalies are determined relative to the RTD2 monthly climatology that is computed from RTD2 over the five-year period. RTD1 dynamic height is very similar to RTD2 dynamic height, and is not discussed here.

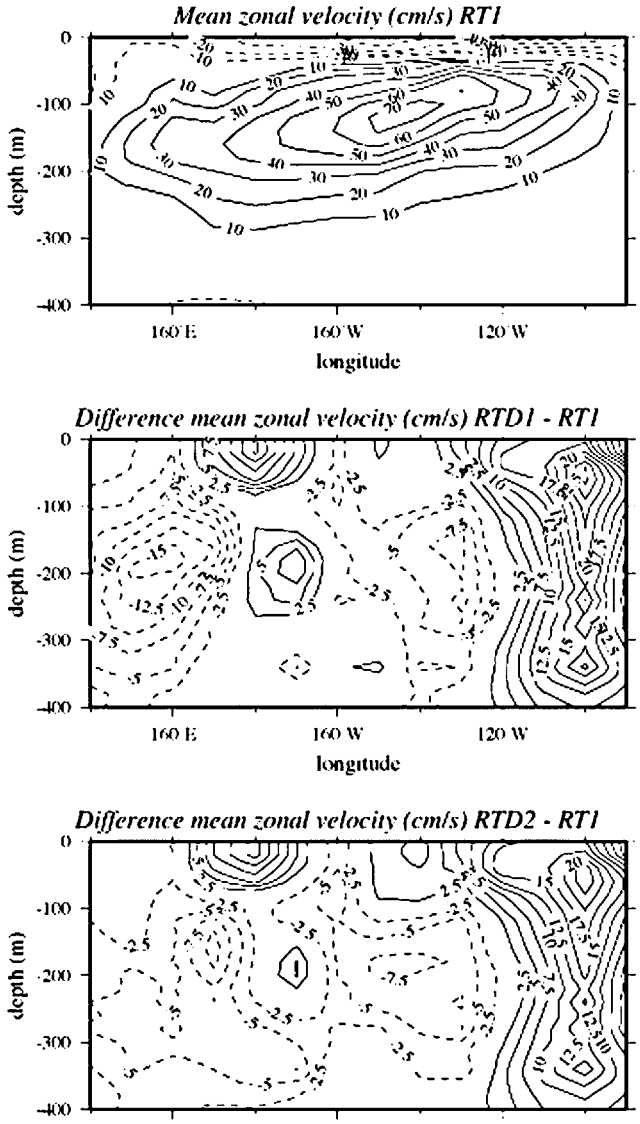

Figure 4. Zonal mean velocity along the equator for RT1 (upper panel). The RTD1−RT1 difference is given in the center panel, the RTD2−RT1 difference is given in the lower panel.

[27] The dynamic height along the equator reflects the evolution of the El Niño and La Niña events, as can be seen through comparison of the dynamic height Hovmüllers with the Southern Oscillation Index (SOI), depicted in the right panel of Figure 6. The analysis starts with the El Niño of 1993, during which dynamic height is anomalously high in the eastern Pacific (more than 5 cm). In both RTD2 and RT1 the dynamic height anomaly reaches a maximum in April. The anomaly weakens, and the conditions change into a weak La Niña. The negative dynamic height anomaly in the eastern Pacific associated with this La Niña is weaker in RTD2 than in RT1. On the other hand, the amplitude of the positive dynamic height anomaly of the successive 1994 El Niño is larger in RTD2 than in RT1.

[28] The negative dynamic height anomaly that crosses the basin in 1995 is weakened in RTD2. The 1995 minimum in the western Pacific is around 6 cm for RTD2, while in RT1 this is 12 cm. In July 1995, a positive height anomaly develops in both runs, which moves eastward in late 1996. In mid-1996, a notable difference in dynamic height between the two runs is found: the assimilation of T/P observations in RTD2 weakens the western Pacific dynamic height anomalies by more than 5 cm.

[29] The difference between the two dynamic height evolutions along the equator is shown in the center-right panel of Figure 6. There is a remarkable contrast between the years 1993, 1994 and 1995 (positive differences) and 1996 and 1997 (negative differences). Dynamic height differences are smaller in the eastern equatorial Pacific than in the western equatorial Pacific.

4.2. Upper Ocean Heat and Salt Content Variability

[30] In RTD2, dynamic height differences are largely due to differences in salinity content as a result of the salinity correction. This is confirmed by a comparison of the heat- and salt content of the upper 550 meters of RT1 and RTD2 (not shown). The differences in salt content between the RTD2 and RT1 is largest for the year 1996 (up to 0.5 psu in the upper layers), and accounts for a dynamic height difference of around 5 cm. A corresponding height difference would correspond to temperature changes of the order of 2.5°C over a layer of around 100 meters thick, centered on the thermocline.

[31] Figure 7 illustrates the differences in heat- and salt content along the equator between RTD2 and RTD1. While RTD2 has the freedom to partition the density correction

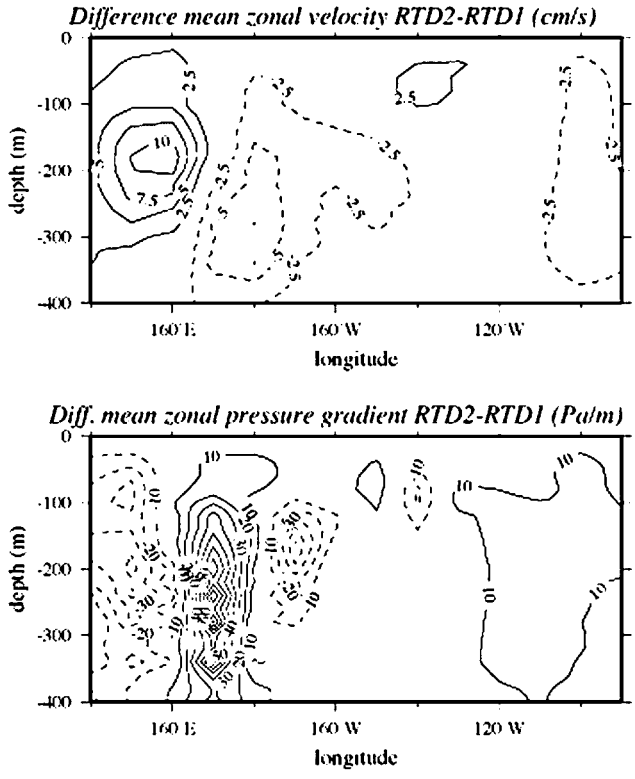

Figure 5. Top panel: zonal mean velocity difference along the equator for RTD2 minus RTD1. Bottom panel: difference in zonal pressure gradient along the equator for RTD2 minus RTD1 (computed from monthly output fields).

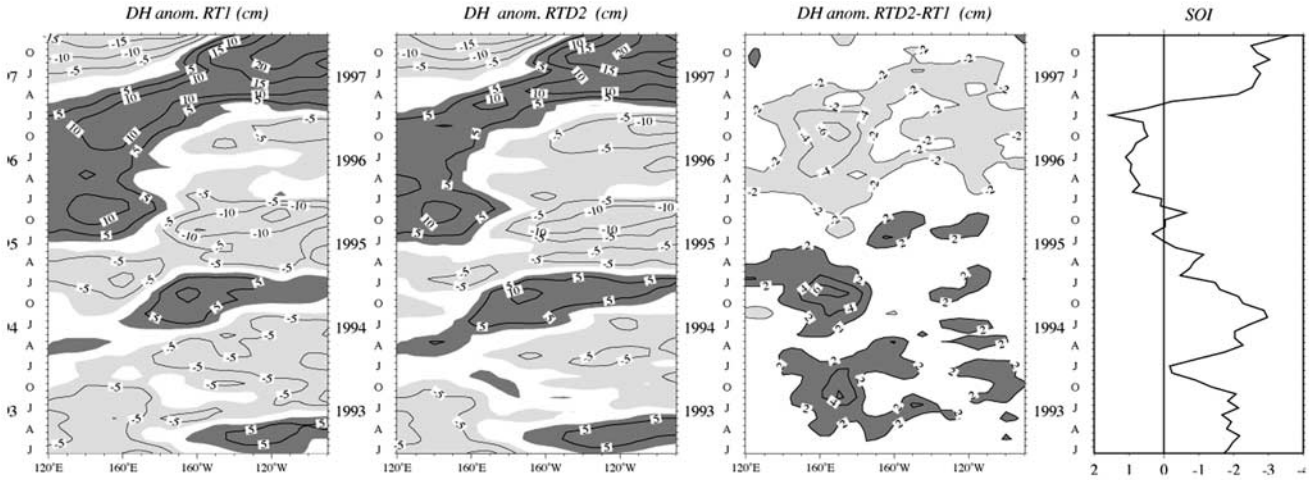

Figure 6. Left and center-left: Longitude–time plot of dynamic height anomalies along the equator for RT1 and RTD2. Contours are drawn every 5 cm. Values greater than 2 cm are shaded dark grey, values lower than −2 cm are shaded light grey. Center-right: difference between the dynamic height anomalies of RTD2 and RT1. Contours are drawn every 2 cm. Shading is identical to the left and center panels. The right panel presents the Southern Oscillation Index, the normalized pressure difference between Tahiti and Darwin. A low value of the SOI and a high value of dynamic height is associated with El Niño conditions, a high SOI with La Niña conditions. Note that the sign of the axis is reversed, in order to facilitate comparison with Figure 11.

between temperature and salinity, RTD1 can only correct density through temperature. As a consequence a compromise has to be made in RTD1 between the temperature correction imposed by the temperature data and the temperature correction required by the sea level information. For 1996, the relatively small density correction required by the sea level observations does not correspond to the relatively large temperature correction required by the temperature observations. As RTD1 can only correct density with temperature corrections, its temperature field is relatively

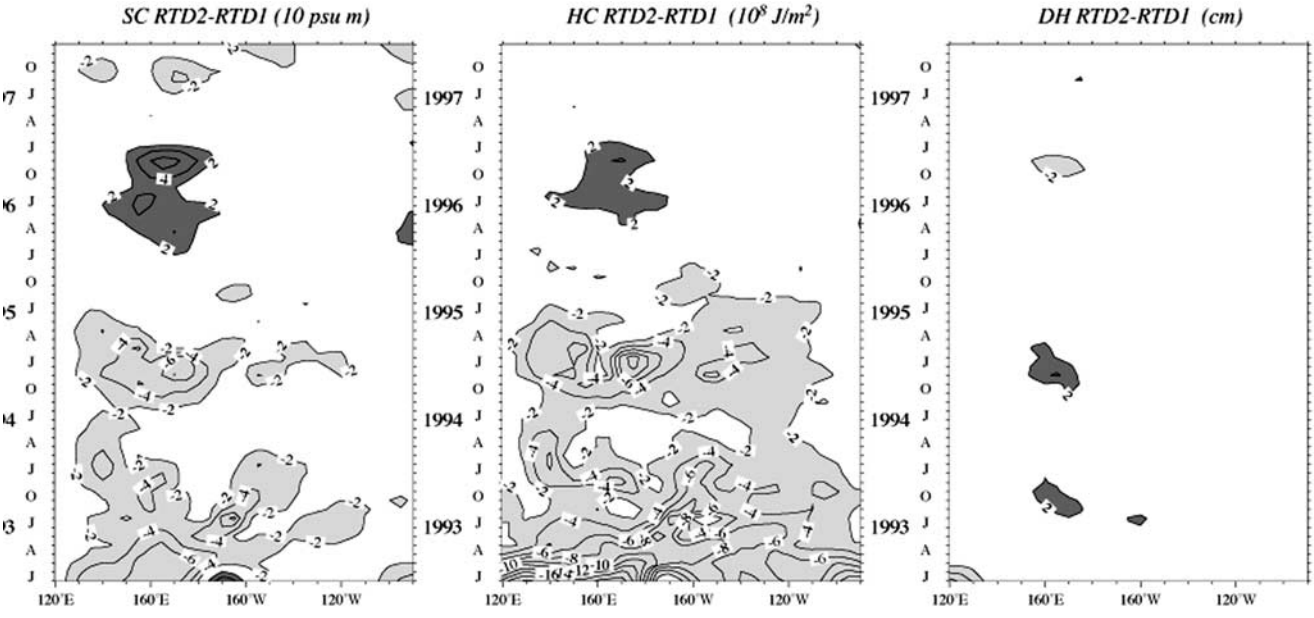

Figure 7. Left: Longitude–time plot of salt content difference in the upper 550 meters along the equator for RTD2 and RTD1. Contours are drawn every 20 psu m. Values greater than 20 psu m are shaded dark grey, values lower than −20 psu m are shaded light grey. Center: difference between the heat content in the upper 550 meters of RTD2 and RT1. Contours are drawn every 2 10^8 J/m^2. Values greater than 2 10^8 J/m^2 are shaded dark grey, values lower than −2 10^8 J/m^2 are shaded light grey. Right: RTD2−RTD1 difference in dynamic height relative to 550 meters depth. Contours are drawn every 2 cm. Values greater than 2 cm are shaded dark grey, values lower than −2 cm are shaded light grey.

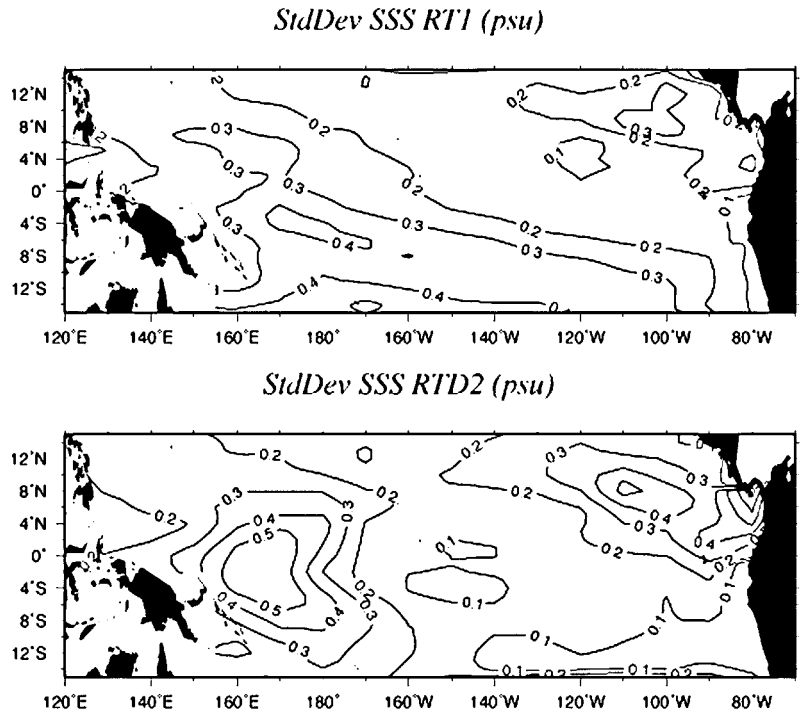

Figure 8. Standard deviation of sea surface salinity computed for the period 1993–1997 for RT1 (top) and RTD2 (bottom).

further removed from temperature observations than is the case in RTD2. Consequently, the heat content of RTD1 is around 3 10^8 J/m^2 lower than of RTD2 to arrive at a sea level that is 2 cm higher, and further removed from T/P observations than RTD2 sea level. The better agreement of RTD2 with both T/P and temperature observations can be explained by the increased number of degrees of freedom in the bivariate scheme, allowing to match the sea level data without compromising the match to the temperature observations.

4.3. Surface Salinity Variability

[32] The variability of SSS is illustrated in Figure 8, which has been made using the same observations as in Figure 2. Compared to RT1, standard deviation of salinity is most noticeably increased (to 0.55 psu) at the salinity front near the date-line, where displacements of the fresh pool cause considerable SSS variability. Also near the coast of Costa Rica the SSS variability has increased as a result of the salinity correction (to a maximum of 0.6 psu). RTD1 SSS is very similar to RT1, and is therefore not discussed separately.

[33] Comparing these results to the observational analyses of *Delcroix et al.* [1996], we observe that the standard deviation in the eastern Pacific corresponds quite well with the values derived from SSS observations. In the western Pacific, however, RTD2 SSS variability is larger than in the work of *Delcroix et al.* [1996]. Part of this variability is related to the meandering of the overestimated strength of the salinity front, discussed in section 3.2.

4.3.1. Sea Surface Salinity EOFs

[34] The modifications in SSS are further analyzed with Empirical Orthogonal Functions (EOFs) with respect to the annual mean state. The first and second EOFs of RTD2 and RT1 are depicted in Figures 9 and 10. Although *Delcroix et al.* [1996] used a different data set than ours for their EOF analysis, and limited their analysis to the region between 140°E and 140°W, the first and second EOFs of RTD2 more closely resemble the observational EOFs [*Delcroix et al.*, 1996, Figures 6 and 7] than do the first and second EOFs of RT1.

[35] The first EOF of SSS in RT1 explains 40 percent of the total variance. The spatial pattern of this EOF shows a North-East/South-West contrast, with maxima centered around 4°N, 80°W and 8°S, 160°W. The first EOF in RTD2 explains also 40 percent of the total SSS variance in RTD2. Its spatial pattern has a clear signature of the western Pacific fresh pool. Maxima are located around 4°S, 160°E, and 4°N, 100°W. For both EOFs, the time evolution of the principal components bears a resemblance with the SOI. This is clear when comparing the SOI in Figure 6 with the principal components of the first EOFs.

[36] The second EOF in RT1 explains 20 percent of the total variance and the second EOF in RTD2 22 percent. Both spatial structures show a North-South contrast. In RTD2, the zero-amplitude contour is directed North-West to South-East whereas in RT1 it is more zonal. The time series for both principal components show a seasonal cycle.

4.3.2. Sea Surface Salinity Variability Along the Equator

[37] The zonal displacements of the fresh pool are illustrated in Figure 11 (computed with the monthly averages of the binned data described above). Zonal displacements of the salinity front are known to correlate well with the SOI [*Delcroix and Picaut*, 1998], and indeed the correlation with the SOI in Figure 6 is evident. A low value of the SOI

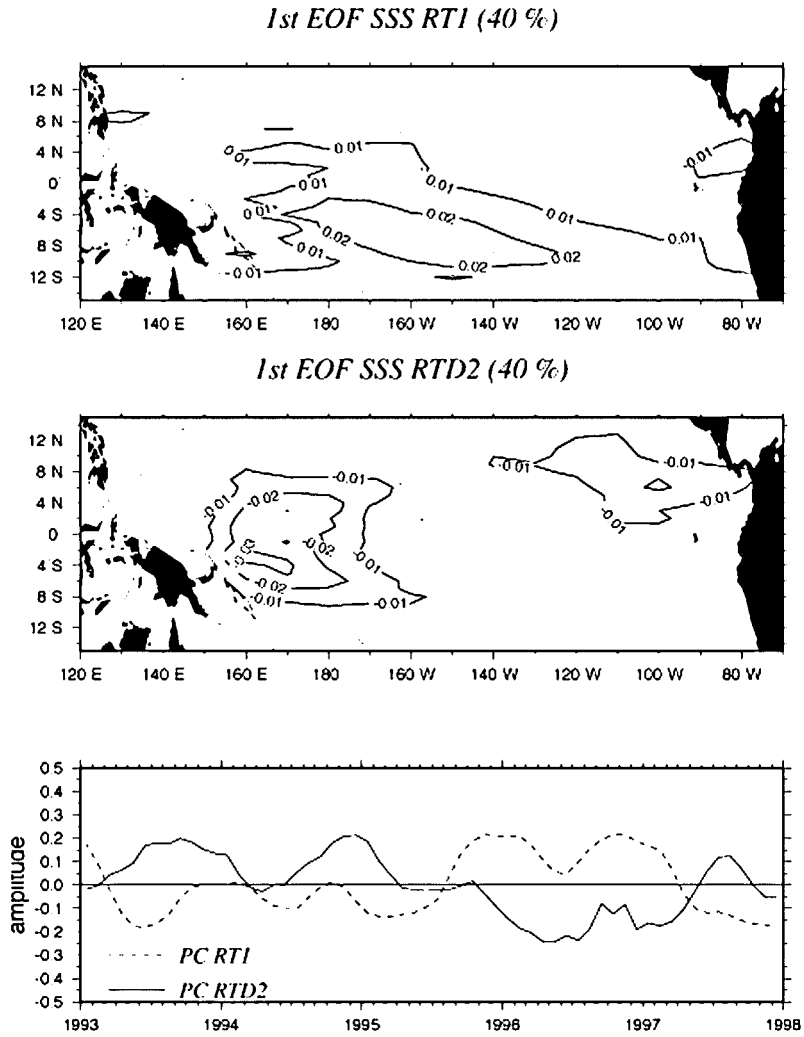

Figure 9. First EOF for SSS in RT1 (top) and RTD2 (center), and the corresponding principal components (bottom).

corresponds to an eastern position of the salinity front (El Niño conditions), while a high SOI corresponds to a western position of the salinity front (La Niña conditions).

[38] Many of the interannual salinity changes in the observations are reproduced by the model runs. As the salinity in RT1 is relaxed to climatological T–S relationships, and no salinity corrections are applied, the salinity changes in this run are generally smaller than in RTD2. To evaluate the variability of SSS in both runs, the root-mean square (RMS) of observed SSS deviations from mean is compared to the RMS values of the SSS deviations derived from the model fields. Before subtracting the mean and computing the RMS values, the model fields have been subsampled at the same times and locations as the observations. The results of the RMS comparison are presented in Figure 12, which shows that in general the SSS variability is underestimated in both model runs. However, as mentioned in section 3.2, SSS variability is overestimated near the salinity front (around 165° E). At times, RTD2 simulates values larger than 35.4 psu and lower than 33.8 psu, which are very uncommon in the observations of this region.

[39] To concentrate on variability rather than on the changes in mean state (sharpening salinity front), we subtracted the model's mean seasonal cycle from the monthly SSS values (not shown). The most striking feature of these interannual anomalies is a positive salinity anomaly in 1996 around 165°E, which corresponds to the dynamic height minimum in Figure 6. This anomaly coincides with the difference in dynamic height between the NCEP analysis with T/P data assimilation and the NCEP analysis without, as discussed by *Ji et al.* [2000]. They argued that this anomaly was due to an underestimation of salinity variability. Comparison between RT1 and RTD2 (and RTD1) demonstrates that the T–S relaxation in RT1 alone (which has not been applied in either of the NCEP analyses) is insufficient to compensate for the difference in height: dynamic height in RT1 (where S is relaxed to T–S relations) is still 6 cm lower than in RTD2 (and RTD1, compare to the 9 cm height discrepancy in Figure 1 of *Ji et al.* [2000]).

[40] To further quantify which of the salinity fields is closer to the observations, we computed the overall correlations of the SSS deviations from mean in RTD2 and RT1

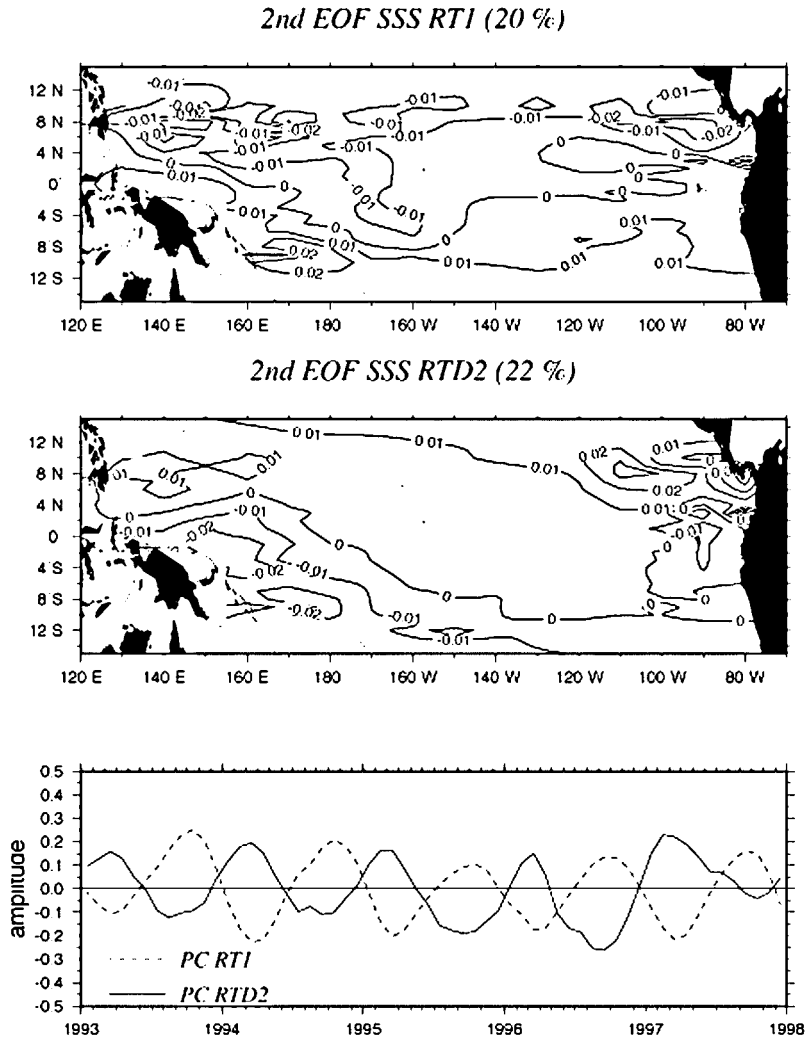

Figure 10. Second EOF for SSS in RT1 (top) and RTD2 (center), and the corresponding principal components (bottom).

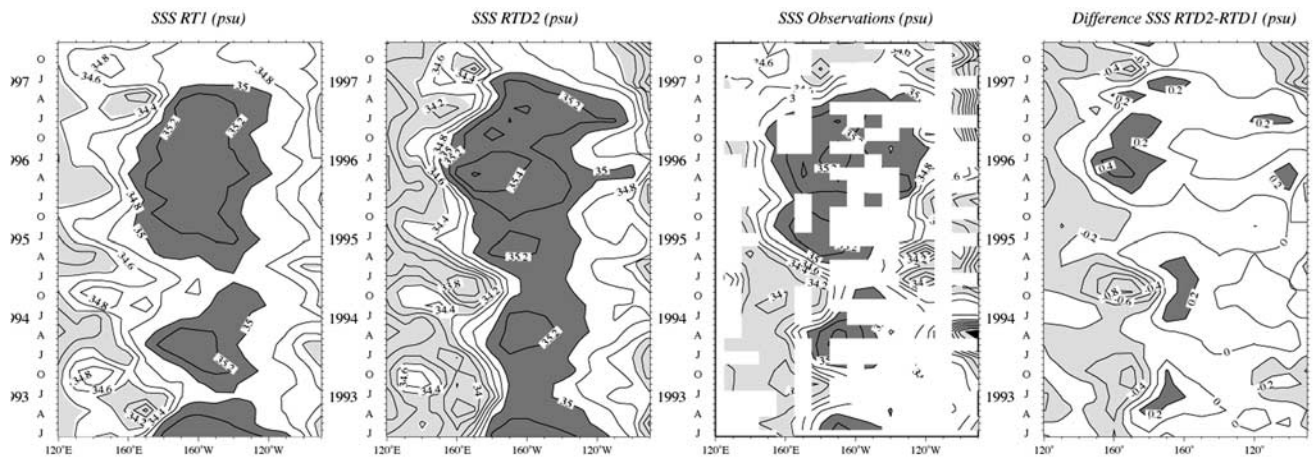

Figure 11. Longitude–time plot of sea surface salinity along the equator. Salinity below 34.4 psu is light grey, salinity greater than 35.0 dark grey. The time axis starts in January 1993, and ends in December 1997. The letters J, A, J and O denote January, April, July and October, respectively.

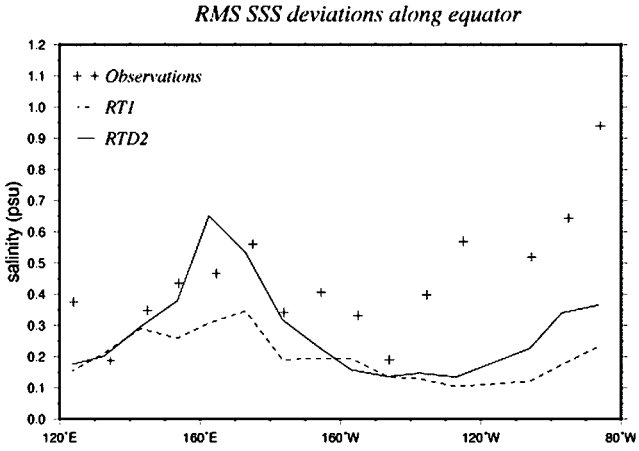

Figure 12. RMS of SSS deviations along the equator as a function of longitude. The crosses denote the RMS of the observed SSS deviations, the dashed line of the SSS deviations in the model run with the assimilation of temperature data (RT1), and the solid line denotes the RMS of the SSS deviations in the bivariate model run in which both temperature and sea level data have been assimilated (RTD2).

with the SSS deviations from mean in the observations (where the model mean is computed by subsampling the model at the time and place of the observations). For RTD2, the correlation for the period 1993–1996, computed at the observation locations, is 64%, for RT1 60%. If we limit the computation of the correlation to the region west of 150°W, the correlation for RTD2 is 75% and the correlation for RT1 64%. The significance of the difference in correlation was investigated with a Monte Carlo test, using an estimate of the number of the degrees of freedom of the salinity field of 40–60, a number that is based on the spatial and temporal correlation scales. Taking into consideration the correlation between RT1 and RTD2 (87%), the difference over the western Pacific is significant at a 95% confidence level, while the difference over the entire equator is not. Based on our statistical analysis, we conclude that in the fresh pool region, the equatorial SSS variability in RTD2 is closer to the observations than in RT1.

4.4. Zonal Velocity Variability at the Surface

[41] Figure 13, a Hovmüller diagram of zonal wind stress compared to zonal currents, shows that the zonal displacements of the salinity front appear to be closely related to changes in zonal wind stress, which is in agreement with the results of *Delcroix and Picaut* [1998]. Qualitatively, the model surface velocity suggests an advection of the salinity front: at 165°E eastward surface velocities are associated with a freshening of the surface waters, while westward surface velocities are associated with an increase in salinity. This can be seen by following the 35.0 psu isohaline, which is plotted in the left panel of Figure 13 (cf. Figure 11).

[42] At the surface, RTD2-RT1 differences are much larger than RTD2-RTD1 differences. Comparison of the RT1 and RTD2 panels of Figure 13 shows that the salinity correction diminishes the amplitude of the surface currents. The westwards currents in the central and eastern Pacific are generally weaker, and so are the eastward currents in response to the westerly wind bursts in the months of January of 1993, 1994, and 1995.

[43] The changes in zonal surface current around 110°W in the first three years of the assimilation are related to the changes in surface pressure. It is remarkable that the months where surface anomalies are positive (weaker SEC) coincide with those months where the impact of data assimilation on the EUC in the eastern Pacific is relatively strong (similar effect as is illustrated for the mean state in Figure 4). While the salinity corrections over the "low salinity" period 1993–1995 cause a considerable change in surface velocities, the surface velocity changes for the corrections in the "high salinity" period 1996–1997 remain relatively small.

4.5. Zonal Velocity Variability Along the EUC

[44] As discussed in section 3.4, the impact of salinity corrections on zonal currents manifests itself mostly below the surface. To investigate the impact of salinity changes on

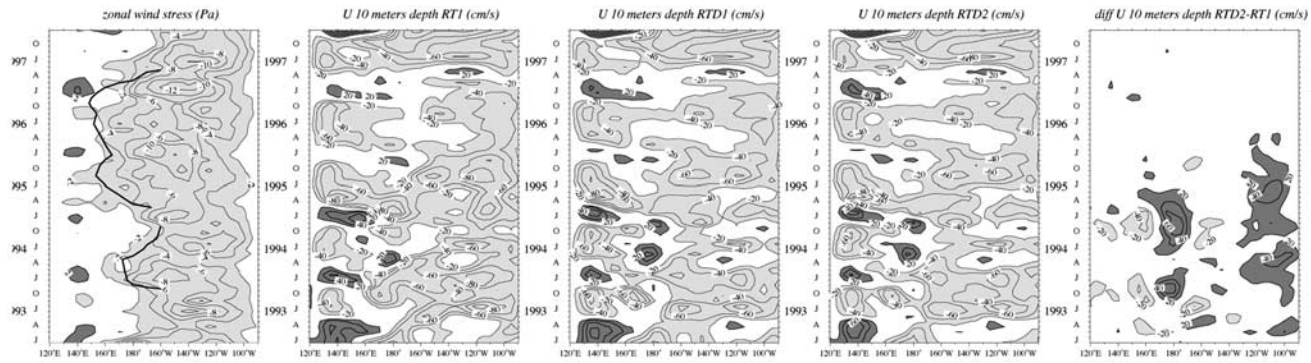

Figure 13. Left: Longitude-time plot of zonal wind stress along the equator (wind-stress product of *Stricherz et al.* [1992]). Contour interval is every 2 Pa, values under −2.0 Pa are shaded light grey, values over 2.0 Pa dark grey. The thick, solid line is the 35.0-psu isohaline based on the surface salinity observations. Center three panels and right panel: longitude–time plot of zonal current at a depth of 10 meters for RT1, RTD1, and RTD2, and the difference between RTD2 and RT1. Contour interval is every 20 cm/s, values below −20.0 cm/s are shaded light grey, values above 20.0 cm/s dark grey.

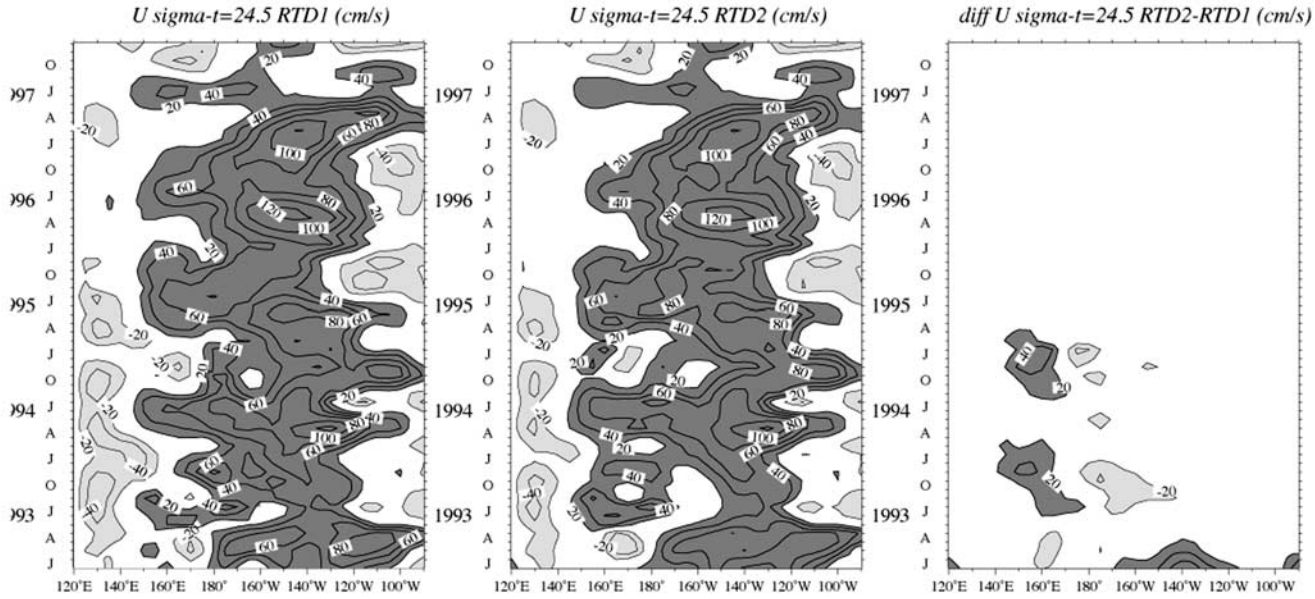

Figure 14. Left: Zonal velocity at sigma-t 24.5 kg/m^3, along the equator. Left: RTD1, center: RTD2, right: difference RTD2−RTD1. Contour interval is every 20 cm/s, values below −20.0 cm/s are shaded light grey, values above 20.0 cm/s dark grey.

the EUC, the zonal velocity at sigma-t level of 24.5 kg/m^3 is plotted in Figure 14. The acceleration west of 160°E, as illustrated in Figure 5 occurs at times of the eastward displacements of the fresh pool in November 1993 and January 1995. For these months, we observe a strengthening of the surface salinity front in RTD2, which results in a different zonal pressure gradient at EUC depth than is the case in RTD1, where all density corrections are made at the thermocline.

5. Summary and Discussion

[45] A bivariate assimilation method has been used and evaluated that uses in situ temperature and altimetric sea level observations to correct model temperature and salinity [*Vossepoel and Behringer*, 2000]. In this method, salinity corrections are applied primarily at the surface layers and temperature corrections at thermocline depth. Compared to a univariate assimilation scheme that assimilates the same observations to correct temperature only, this leads to a different upper ocean salinity field, a different vertical distribution of density corrections, and hence to a different velocity field.

[46] Whether applying the univariate scheme or the bivariate scheme, the assimilation of T/P observations affects the simulation of dynamic height anomalies during the 1993–1997 period. In the bivariate run, where both temperature and salinity are corrected, the assimilation results in a more realistic salinity variability in the western Pacific than in two univariate runs (one with both sea level and temperature data and one with only temperature data). Specifically the salinity gradient at the eastern edge of the fresh pool is sharpened in the bivariate run. EOF analyses of model simulation of SSS illustrates that the primary impact of the T/P assimilation in the bivariate run is the reproduction of the zonal displacements of the salinity front.

[47] The overcorrection of salinity is likely to be related to the fact that we relate T/P observations to a different reference level than the model dynamic height estimations. In theory, it would be better to relate the total sea level observations to the total dynamic height estimations, but that would require a more accurate estimate of the geoid. The planned GOCE mission will provide such an estimate.

[48] By assuming that dynamic height differences between T/P observations and those derived from temperature observations are mainly due to salinity variations, we may have introduced some spurious salinity anomalies. In the first place, it is very well possible that we underestimated observational errors. Altimeter observations are corrected for meteorological conditions (e.g., wet tropospheric correction). Errors in these corrections may be correlated in time and space, but the assimilation scheme does not take these correlations into account. Secondly, errors may be introduced by the fact that we neglect barotropic signals by setting variations of dynamic height down to 500 meters depth equivalent to sea level variations.

[49] The bivariate scheme has a higher number of degrees of freedom, which permits a solution that is closer to both the temperature and the altimeter observations. The consequences are especially noteworthy for the 1996 La Niña, where the bivariate scheme applies a positive salinity correction and a relatively large temperature correction while the univariate scheme only slightly corrects temperature, in order to match the observed sea level.

[50] By changing surface pressure, the assimilation of T/P affects velocity both at the surface and below. Both assimilation runs that assimilate sea level observations have an EUC that extends further eastward and to greater depth in the eastern Pacific. This might depend on the type of data assimilation method used. In data assimilation systems of the type used here, the assimilation procedure changes the density field through changes in temperature and/or salinity.

The corresponding velocities are not corrected although model density errors and model velocity errors are correlated. Consequently, improving density by data assimilation can in some situations make equatorial zonal velocities actually worse. A possible solution to this problem is to include velocity corrections in geostrophic balance with the density corrections, as discussed by G. Burgers et al. (Balanced ocean-data assimilation near the equator, submitted to *Journal of Physical Oceanography*, 2002).

[51] The implication of salinity corrections on zonal currents is most evident at the EUC, in particular during the El Niño episodes of 1993 and 1995. West of 160°E, the bivariate run has a relatively weaker zonal pressure gradient at thermocline depth than the univariate run, and consequently the EUC in the bivariate run is accelerated differently than in the univariate run.

[52] The simulation of surface currents in the model is not significantly improved by the salinity correction. The relative impact of temperature and salinity corrections is a tunable parameter in our assimilation system. The results of the current paper suggest that although this parameter might require further tuning, the zonal velocity effects along the equator in the eastern Pacific are not very sensitive to this parameter.

[53] Another possible source of velocity errors may be the wind-stress forcing, which has a considerable uncertainty. Furthermore, the model has been forced with monthly forcing fields, while for a proper simulation of the adjustment of currents in the tropical Pacific ocean a weekly wind forcing would be more appropriate. Such forcing includes high frequency variations such as westerly wind bursts, which are believed to play an important role in the onset of El Niño [e.g., *Lengaigne et al.*, 2002].

[54] Considering the 1993–1997 analysis presented above, our results indicate that the combination of temperature and sea level data in the bivariate assimilation scheme leads to a more realistic model representation of the salinity front at the eastern edge of the fresh pool. In addition, the combination of temperature and salinity corrections allows an estimation of heat content that is closer to the temperature observations than in a univariate scheme that assimilates the same observations. The salinity corrections in the western Pacific result in this region in a more westward acceleration of the EUC compared to the case when only temperature corrections are applied. Surface zonal velocity changes in the bivariate run are not directly related to the salinity corrections, but rather to the change in sea surface pressure. For an improved simulation of the surface currents, our results stress the importance of a well-defined reference level for the altimeter observations, of a high-quality wind-stress forcing product and of a data-assimilation scheme that treats velocity adequately. The combined development of all these aspects may be essential for further improvements of the NCEP forecasts.

[55] **Acknowledgments.** The authors wish to thank Bob Cheney for providing the altimeter data. The thermosalinograph data were kindly provided by Christian Hénin, the CTD observations by Mike McPhaden. The mooring and ADCP data were obtained through the Web site of the Pacific Marine Environmental Laboratory, for which we acknowledge Mike McPhaden. We acknowledge Gary Lagerloef for kindly providing the zonal surface velocity estimates. The help of Ming Ji, Dick Reynolds, Dave Behringer and Christophe Maes has been essential for using and adapting the analysis system of the Climate Modeling Branch of the National Center of Environmental Prediction. This is gratefully acknowledged. The suggestions of two anonymous reviewers have helped improving the manuscript. Femke Vossepoel wishes to thank her colleagues at LODYC for valuable discussions. Computing resources were provided by the Center for High Performance applied Computing (HPαC) of Delft University of Technology. This project is funded by the Space Research Organization Netherlands, SRON EO-024. Peter Jan van Leeuwen was supported by the National Research Program on Global Change NOP II, grant 013001237.10.

References

Acero-Schertzer, C. E., D. V. Hansen, and M. S. Swenson, Evaluation and diagnosis of surface currents in the NCEP ocean analyses, *J. Geophys. Res.*, *102*, 21,037–21,048, 1997.

Ando, K., and M. J. McPhaden, Variability of surface layer hydrography in the tropical Pacific ocean, *J. Geophys. Res.*, *102*, 23,063–23,078, 1997.

Behringer, D., M. Ji, and A. Leetmaa, An improved coupled model for ENSO prediction and implications for ocean initialization, 1, The ocean data assimilation system, *Mon. Weather Rev.*, *123*, 1013–1021, 1998.

Bryan, K., A numerical model for the study of the circulation of the world ocean, *J. Comput. Phys.*, *4*, 347–376, 1969.

Cooper, N. S., The effect of salinity in tropical ocean models, *J. Phys. Oceanogr.*, *18*, 697–707, 1988.

Cox, M. D., A primitive, 3-dimensional model of the ocean, *GFDL Ocean Group Tech. Rep. 1*, Geophysical Fluid Dynamics Laboratory/NOAA, Princeton Univ., Princeton, N. J., 1984.

Cronin, M. F., and M. J. McPhaden, Upper ocean salinity balance in the western equatorial Pacific, *J. Geophys. Res.*, *103*, 27,567–27,587, 1998.

Delcroix, T., and J. Picaut, Zonal displacement of the western equatorial Pacific "fresh pool", *J. Geophys. Res.*, *103*, 1087–1098, 1998.

Delcroix, T., C. Hénin, V. Porte, and P. Arkin, Precipitation and sea-surface salinity in the tropical Pacific Ocean, *Deep Sea Res.*, *43*, 1123–1141, 1996.

Derber, J., and A. Rosati, A global oceanic data assimilation system, *J. Phys. Oceanogr.*, *19*, 1333–1347, 1989.

Godfrey, J. S., and E. J. Lindstrom, The heat budget of the equatorial western Pacific surface mixed layer, *J. Geophys. Res.*, *94*, 8007–8017, 1989.

Halpern, D., Y. Chao, C.-C. Ma, and C. R. Mechoso, Comparison of tropical Pacific temperature and current simulations with two vertical mixing schemes embedded in an ocean general circulation model and reference to observations, *J. Geophys. Res.*, *100*, 2515–2522, 1995.

Halpern, D., M. Ji, A. Leetmaa, and R. W. Reynolds, Influence of assimilation of subsurface temperature measurements on simulations of Equatorial Undercurrent and South Equatorial Current along the Pacific equator, *J. Atmos. Oceanic Technol.*, *15*, 1471–1477, 1998.

Hénin, C., Y. du Penhoat, and M. Ioualalen, Observations of sea surface salinity in the western Pacific fresh pool: Large-scale changes in 1992–1995, *J. Geophys. Res.*, *103*, 7523–7536, 1998.

Ji, M., A. Leetmaa, and J. Derber, An ocean analysis system for seasonal to interannual climate studies, *Mon. Weather Rev.*, *123*, 460–481, 1995.

Ji, M., R. W. Reynolds, and D. Behringer, Use of TOPEX/Poseidon sea level data for ocean analysis and ENSO prediction: Some early results, *J. Clim.*, *13*, 216–231, 2000.

Kalnay, E., et al., The NCEP/NCAR 4-year reanalysis project, *Bull. Am. Meteorol. Soc.*, *77*, 437–471, 1996.

Lengaigne, M., J.-P. Boulanger, C. Menkes, S. Masson, G. Madec, and P. Delecluse, Ocean response to the March 1997 westerly wind event, *J. Geophys. Res.*, *107*, doi:10.1029/2001JC000841, in press, 2002.

Levitus, S., and T. P. Boyer, *World Ocean Atlas 1994*, Vol. 4, *Temperature*, vol. NOAA Atlas NESDIS 3, U.S. Dep. of Commer., Washington D. C., 1994.

Levitus, S., R. Burgett, and T. P. Boyer, *World Ocean Atlas 1994*, Vol. 3, *Salinity*, vol. NOAA Atlas NESDIS 3, U.S Dep. of Commer., Washington D. C., 1994.

Lukas, R., and E. R. Lindstrom, The mixed-layer of the western equatorial Pacific ocean, *J. Geophys. Res.*, *96*, 3343–3357, 1991.

Maes, C., and D. Behringer, Using satellite-derived sea level and temperature profiles for determining the salinity variability: A new approach, *J. Geophys. Res.*, *104*, 8537–8547, 2000.

Maes, C., D. Behringer, R. W. Reynolds, and M. Ji, Retrospective analysis of the salinity variability in the western tropical Pacific Ocean using an indirect minimization approach, *J. Atmos. Oceanic. Technol.*, *17*, 512–524, 2000.

Murtugudde, R., and A. Busalacchi, Salinity effects in a tropical ocean model, *J. Geophys. Res.*, *103*, 3283–3300, 1998.

Pacanowski, R. C., and S. G. H. Philander, Parameterization of vertical mixing in numerical models of tropical oceans, *J. Phys. Oceanogr.*, *11*, 1443–1451, 1981.

Philander, S., W. J. Hurlin, and A. D. Siegel, A model of the seasonal cycle in the tropical Pacific Ocean, *J. Phys. Oceanogr.*, *17*, 1986–2002, 1987.

Roemmich, D., M. Morris, W. R. Young, and J. R. Donguy, Fresh equatorial jets, *J. Phys. Oceanogr.*, *24*, 540–558, 1994.

Shinoda, T., and R. Lukas, Lagrangian mixed layer model of the western equatorial Pacific, *J. Geophys. Res.*, *100*, 2523–2541, 1995.

Stockdale, T. N., A. J. Busalacchi, D. E. Harrison, and R. Seager, Ocean modeling for ENSO, *J. Geophys. Res.*, *103*, 14,325–14,355, 1998.

Stricherz, J., J. J. O'Brien, and D. M. Legler, *Atlas of Florida State University Tropical Pacific Winds for TOGA 1966–1985*, Florida State Univ., Tallahassee, Fla., 1992.

Troccoli, A., and K. Haines, Use of T–S relation in a data assimilation context, *J. Atmos. Oceanic. Technol.*, *16*, 2011–2025, 1999.

Vialard, J., and P. Delecluse, An OGCM study for the TOGA decade, 1, Role of salinity in the physics of the western Pacific fresh pool, *J. Phys. Oceanogr.*, *28*, 1071–1088, 1998a.

Vialard, J., and P. Delecluse, An OGCM study for the TOGA decade, 2, Barrier layer formation and variability, *J. Phys. Oceanogr.*, *28*, 1089–1106, 1998b.

Vialard, J., P. Delecluse, and C. Menkes, A modeling study of salinity variability and its effects in the tropical Pacific ocean during the 1993–1999 period, *J. Geophys. Res.*, *107*, doi:10.1029/2001JC000758, in press, 2002.

Vossepoel, F., and D. W. Behringer, Impact of sea level assimilation on salinity variability in the western equatorial Pacific, *J. Phys. Oceanogr.*, *30*, 1706–1721, 2000.

Vossepoel, F., R. W. Reynolds, and L. Miller, The use of sea level observations to estimate salinity variability in the tropical Pacific, *J. Atmos. Oceanic Technol.*, *16*, 1400–1414, 1998.

Wacongne, S., Dynamical regimes of a fully nonlinear stratified model of the Atlantic Equatorial Undercurrent, *J. Geophys. Res.*, *94*, 4801–4815, 1989.

Wacongne, S., On the difference in strength between the Atlantic and Pacific undercurrent, *J. Phys. Oceanogr.*, *20*, 792–799, 1990.

Xie, P., and P. A. Arkin, Global precipitation: A 17-year monthly analysis based on gauge observations, satellite estimates and numerical model outputs, *Bull. Am. Meteorol. Soc.*, *78*, 2539–2558, 1997.

F. C. Vossepoel, University Pierre et Marie Curie, 4, Place Jussieu, 75252 Paris Cedex 05, France. (Femke.Vossepoel@lodyc.jussieu.fr)

G. Burgers, Royal Netherlands Meteorological Institute (KNMI), De Bilt, Netherlands.

P. J. van Leeuwen, Institute for Marine and Atmospheric Research Utrecht (IMAU), Utrecht University, Utrecht, Netherlands.